BJR

https://doi.org/10.1259/bjr.20170681

Received: 09 September 2017 | Revised: 03 June 2018 | Accepted: 04 July 2018

Cite this article as:
Song J, Hu Q, Huang J, Chen T, Ma Z, Shi H. MR targeted imaging for the expression of tenascin-C in cervical cancer . *Br J Radiol* 2018; **91**: 20170681.

FULL PAPER

MR targeted imaging for the expression of tenascin-C in cervical cancer

[1]JIACHENG SONG, MD, [2]QIMING HU, MD, [1]JUNWEN HUANG, MD, [1]TING CHEN, PhD, [1]ZHANLONG MA, PhD and [1]HAIBIN SHI, PhD

[1]Department of Radiology, The First Affiliated Hospital of Nanjing Medical University, Nanjing, China
[2]Department of Obstetrics & Gynecology, The First Affiliated Hospital of Nanjing Medical University, Nanjing, China

Address correspondence to: Dr Ting Chen
E-mail: *chentingwzc@163.com; mzlwzcdyx@163.com*

Objective: To detect cervical cancer and compare tumor invasiveness using a molecular targeted probe.
Methods: Tenascin-C expression was evaluated in 15 specimens. Five of them were cervical cancer with node metastasis (group A), five were cervical cancer without node metastasis (group B), and another five were normal cervix tissues (group C). Superparamagnetic iron oxide (SPIO) nanoparticles and tenascin-C antibody were conjugated as an MR probe. After the fresh tissues incubated with the probe for 24 h, MR was performed to analysis the tissue signal changes.
Results: Cervical cancer tissues with node metastasis showed highest tenascin-C expression, while normal cervix showed little expression. For the non-metastatic cervical cancer patients, tenascin-C showed moderate expression. Tenascin-C was found diffusely in the stromal surrounding malignant tumor cells. After MR, the image signal changes (contrast-to-noise ratio) kept consistent with tenascin-C expression and showed statistical difference between the three groups (A: 3.87 ± 1.45 *vs* B: 2.33 ± 1.04 *vs* C: 0.66 ± 0.31; $p = 0.002$).
Conclusion: Tenascin-C expression can help to detect cervical cancer. MRI with SPIO-antitenascin-C may be used to evaluate the preoperative cervical cancer patients with node metastasis.
Advances in knowledge: Tenascin-C expression can help to detect cervical cancer and compare cancer invasiveness. Protein expression difference can be captured and compared on MR with SPIO-antitenascin-C.

INTRODUCTION

Tenascin-C is an extracellular matrix glycoprotein. It shows little or no expression in healthy adult tissues, but re-expressed upon tumor angiogenesis and metastasis.[1] Tenascin-C concentrations have been associated with numerous aggressive cancers, such as breast cancer,[2] pancreas cancer,[3] glioblastoma[4] and so on. Tenascin-C may alter cell matrix that may facilitate epithelial tumor cell invasion during carcinogenesis.[5] Tenascin-C amino-acid sequence also shows epidermal growth factor-like repetitions, which was related with tumor angiogenesis and metastasis.[6] Thus, tenascin-C is believed to be a multifunctional robust tumor marker.

Tenascin-C has been reported to be higher in invasive cancers than cervicitis and squamous intraepithelial lesions.[7] It represents proliferative activity of the epithelium.[8] For the clinical suspected cervical cancer patients with difficulty in preoperative tumor sampling or negative pathology results, high tenascin-C expression may be important in supporting malignancy.

Lymph node metastasis is very common and important for patients with cervical cancer since it influences 5-year survival rate and affects treatment.[9] Pelvic MR is commonly used to delineate the size, position, and stage of cervical cancer.[10] But the sensitivity and specificity for node metastasis detecting is not very effective.[11] Especially in detecting lymphatic metastasis in normal-sized and normal-shaped nodes.[12] Tenascin-C expression level in cervical cancer patients with lymph node metastasis has not been researched before, but was important and meaningful. Then how to accurately evaluate cervical cancer invasiveness from MR? Functional protein targeted MRI may be further researched.

Therefore, we focused on two main objectives: (1) to compare tenascin-C expression difference among normal cervix and cervical cancer with or without node metastasis (2) to detect the tumor tissue signal changes on MR after incubated with superparamagnetic iron oxide (SPIO)-antitenascin-C.

Figure 1. Flow chart of experiment process. LN, lymph node; SPIO, super paramagnetic iron oxide; TN-C, tenascin-C.

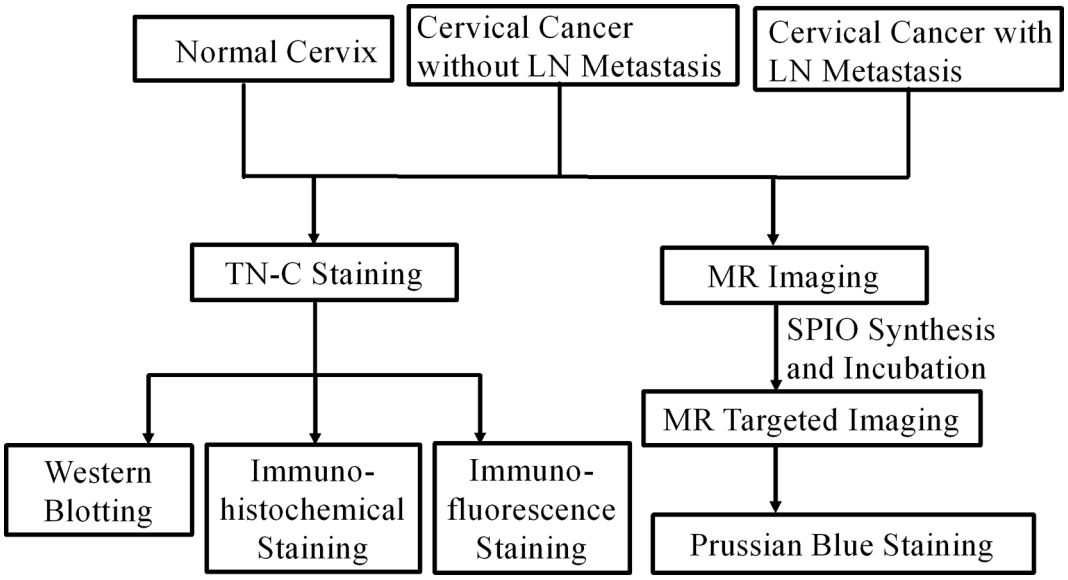

METHODS AND MATERIALS

Patients and tissue samples

After hysterectomy, we cut the tumor tissue of about 1 cm^3 in the middle of the tumor. The same size of tissues were also cut from normal cervix. These samples were divided into three groups: A, cervical cancer with lymph node metastasis; B, cervical cancer without lymph node metastasis; C, normal cervix.

The whole research process was listed in the flow chart (Figure 1).

Histological analysis

These methods were used to verify tenascin-C expression difference:

Western blotting

Tissue were harvested into homogenizer containing protease and phosphatase inhibitors. Protein samples were separated by 10% sodium dodecyl sulfate polyacrylamide gel electrophoresis, then transferred onto polyvinylidene fluoride membranes (Millipore, Billerica, MA), blocked with Tris-Buffered Saline Tween TBST containing 5% skimmed milk for 1 h at 37°C. And reacted with primary antibody rabbit antitenascin-C antibody (1:500, Abcam, Cambridge, MA), and mouse anti-β-actin antibody (1:5000, Abcam, Cambridge, MA). After being washed in TBST at room temperature, visualized with electrochemiluminescence detection kit (Amercontrol Biosciences, London, UK).

Immunohistochemical staining

The primary antibody was rabbit anti rat antitenascin-C. The tissue was covered with 5% bovine serum albumin (BSA) and diaminobenzidine staining for 10 min.

Immunofluorescence staining

The tissue was covered with 5% bovine serum albumin, the primary antibody was rabbit anti rat antitenascin-C (1:200) and anti-CD34 (1:200). After added second antibody 488-Alex (1:400), 4',6-Diamidine-2'-phenylindole DAPI was incubated for 10 min. The red color represent the expression of tenascin-C. The blue color represent tumor cell nucleus.

Prussian blue staining

Prussian blue staining was used to prove the probe existence in the tissues. Perls solution was prepared with 2% sodium cyanide ferrous mixes with 2% hydrochloric acid. After 30 min of staining, the tissue was kept in 0.5% neutral red dye water for 2 min.

Preparation and characteristics of SPIO-antitenascin-C

Fe_2O_3-Dimercaptosuccinic acid (2.7 mg ml^{-1}, 0.2 mg) were added into 10 μl borate saline buffer. 1-(3-dimethylaminopropyl)−3-ethylcarbodiimide hydrochloride (10 mg ml^{-1}) and sulfo-N-hydroxysuccinimide (10 mg ml^{-1}) were added together to a 15 min shaker. 200 mg tenascin-C antibody which has been dialyzed for 48 h and was added and then shacked for 2 h. The characteristics including appearance, Zeta potential, size distribution. The liquid was observed with naked eye and put together with magnetic to show the magnetism characteristic. Zeta potential was measured using instruments (Malvern Instruments, Malvern, UK). The average core size and morphology were observed and measured using transmission electron microscope (TEM-1010, Japan).

MR images acquisition

MRI examinations were performed using a 3.0 T MRI scanner (MAGNETOM TrioTim, Siemens, Erlangen, Germany) with employing 8-channel head phased array coil. Images were obtained with a proton density (PD) weighted images. FOV read was 120 mm, FOV phase was 100%. The images were acquired axis and sagittal view with 1 mm thickness of each slice. The total slices was 18. The echo time was 31 ms, repetition time was 2800 ms.

Each tissue was put in the cryovial. After washed with phosphate buffered saline for three times, they were scanned immediately before incubation.

The synthesized SPIO-antitenascin-C (0.67 mg ml^{-1}, 0.05 ml) was incubated with the fresh tissue for 24 h under 37°C. Then washed with phosphate buffered saline for three times. Then tissues were put in the cryovial and scanned again under the same condition with the same MR sequence.

MRI data processing

Signal intensities were measured manually in our picture archiving and communication systems system, by drawing a region of interest (diameter 5 mm) in the center of the tissue to avoid signal disturbance. Contrast-to-noise ratio (CNR) was calculated as [CNR= (SI_{bef} – SI_{aft})/ SI_{air}], where SI_{bef} represents the signal intensity of tissues before incubation, SI_{aft} represents the signal intensity of tissues after incubated for 24 h, and SI_{air} represents the signal intensity of air as background noise.

Statistical analysis

All data were reported as mean ± standard deviation. All analyses were performed using SPSS18.0 software. Tenascin-C expression comparison and signal changes on MRI use one-way ANOVA and pairwise comparison was conducted if the difference was statistically significant. Statistically significant was considered as $p < 0.05$.

RESULTS

Tenascin-C expression level comparison

Tenascin-C was mainly expressed in the stromal of cervical cancer with lymph node metastasis (Figure 2A1–A3). The white arrow pointed to the tumor and metastatic lymph node (Figure 2A4,A5). For the non-metastatic cervical cancer patients, tenascin-C showed moderate expression (Figure 2B1–B3). The white arrow pointed to the tumor (Figure 2B4). No obvious enlarged metastatic nodes can be seen (Figure 2B5). The normal cervix showed only a little expression (Figure 2C1–C3). Multiple myoma can be seen without enlarged nodes (Figure 2C4,C5). Tenascin-C was found diffusely in the stromal surrounding malignant tumor cells.

Characteristics of SPIO-antitenascin-C

The probe appears to be clear and transparent brown liquid with naked eye, which showed strong magnetic properties when put together with the magnet (Figure 3A). The SPIO-antitenascin-C molecular probe presents with a spherical core shell structure with an average core diameter of 41.3 nm (Figure 3B,C). Fe concentration of probe was 0.67 mg ml^{-1} with 0.02 mg ml^{-1} antibody concentration. The Zeta potential distribution was demonstrated −27.7 mV (Figure 3D).

MR imaging of tenascin-C and statistical analysis

Tissues signal intensity before incubation did not show statistical difference (A: 1.40 ± 0.15 *vs* B: 1.52 ± 0.12 *vs* C: 1.39 ± 0.13) × 10^{-3}; ($p = 0.251$). After incubated with the probe, tumor tissues with

Figure 2. (A) Cervical cancer with node metastasis in 64-year-old females. (B) Cervical cancer without node metastasis in 48-years-old female. (C) Multiple uterine myoma in 40- years-old females with menstrual disorder. (A1, B1, C1) Western blotting of tenascin-C, tissue A presented marked expression. (A2, B2, C2) Immunohistochemical staining of tenascin-C, tissue A and B showed greater cellular density, enlarged nuclei and more tenascin-C expression. (A3, B3, C3) Immunofluorescence staining of the expression of tenascin-C. More tenascin-C expression was seen in tissue A. (A4, B4) White arrow pointed to the tumor. (C4) Multiple myoma can be found. (A5) White arrow pointed to the enlarged metastatic lymph node. (B5, C5) No enlarged lymph node can be seen. TN-C, tenascin-C.

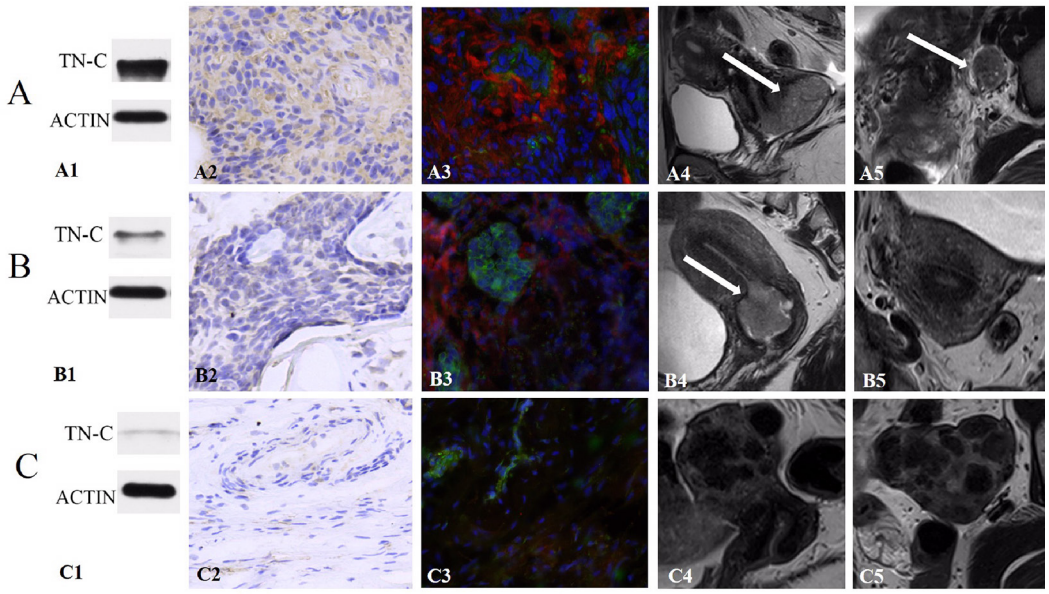

Figure 3.(A) Strong magnetism of the synthesis liquid. (B) The size of the probe is about 42.3 nm. (C) Under the TEM, the probe appears spherical particles, uniform distribution and good dispersibility. (D) The Zeta potential distribution of the probe is −27.7 mV. TEM, transmission electron microscopy.

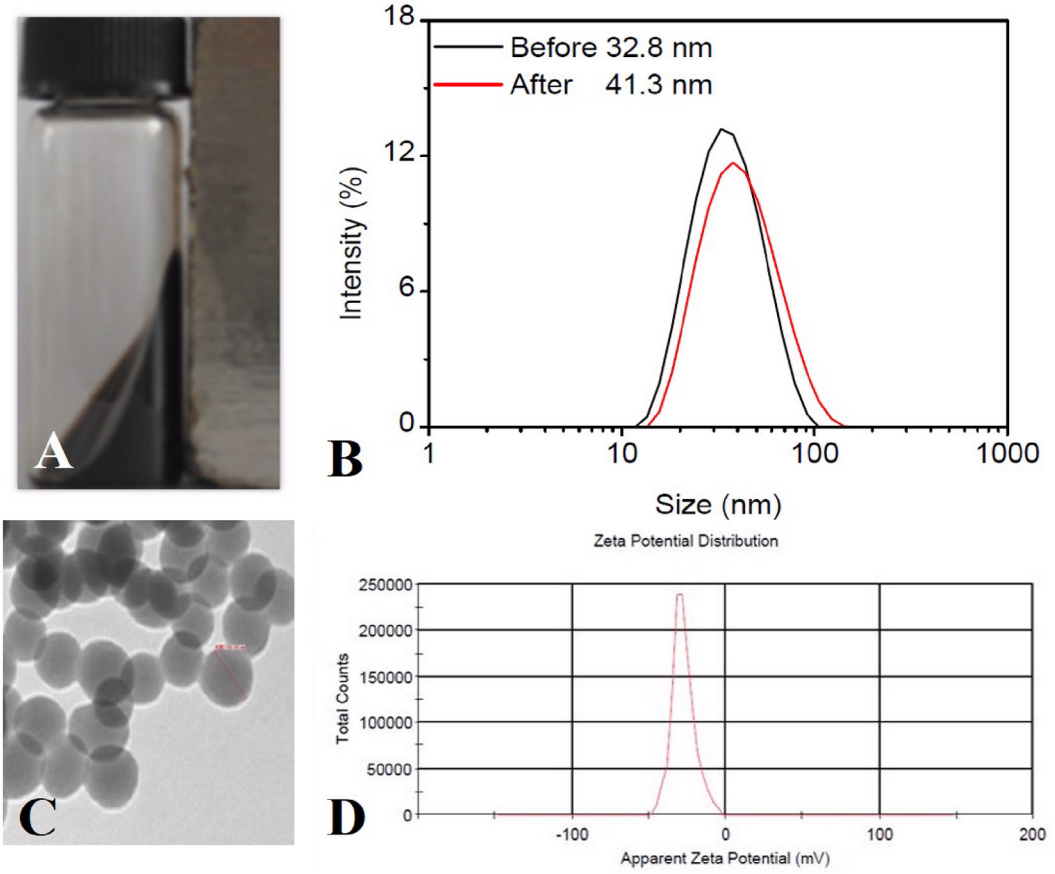

node metastasis showed obvious signal decrease (Figure 4A). Tumor tissues without node metastasis showed moderate signal decrease. Normal cervix showed little signal decrease (Figure 4B). They showed statistical difference between the groups (A: 0.92 ± 0.14 *vs* B: 1.19 ± 0.12 *vs* C: 1.30 ± 0.11) × 10^{-3}; (p = 0.001). The signal decrease CNR was (A: 3.87 ± 1.45 *vs* B: 2.33 ± 1.04 *vs* C: 0.66 ± 0.31; p = 0.002). (Table 1, Figure 5)

Prussian blue staining verified the existence of SPIO inside the tumor tissues (red arrows). More blue dots which stand for

Figure 4. (A) Cervical cancer tissue with node metastasis incubated with the probe for 24 h. The tissue showed marked signal decrease and prussian blue staining verify the existence of targeted probe in the tumor (arrows). (B) Normal cervical tissue incubated with the probe for 24 h. A little signal decrease kept consistent with little dot on prussian blue staining (arrows).

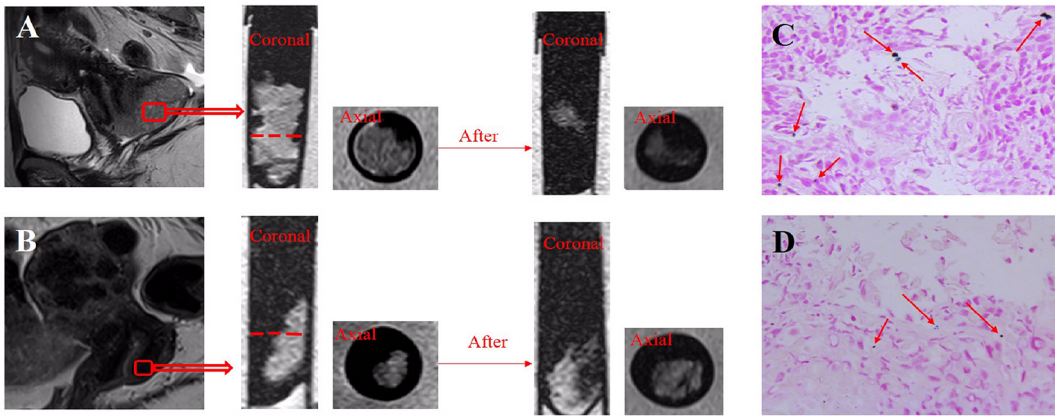

Table 1. Signal decrement comparison on MR images

	Cervical cancer with metastasis	Cervical cancer without metastasis	Normal cervix	*p*-value
SI before ($\times 10^{-3}$)	1.40 ± 0.15	1.52 ± 0.12	1.39 ± 0.13	0.251
SI after ($\times 10^{-3}$)	0.92 ± 0.14	1.19 ± 0.12	1.30 ± 0.11	0.001[a]
CNR	3.87 ± 1.45	2.33 ± 1.04	0.66 ± 0.31	0.002[a]

CNR, contrast-to-noise ratio; SI, signal intensity.
[a]$p < 0.05$

more probes can be find in the tumor tissue than normal cervix. (Figure 4C,D)

DISCUSSION

In our study, the expression of tenascin-C was upregulated in the cervical cancer tissues. Cancer tissues with lymph node metastasis showed much higher expression than non-metastatic tissues. Protein expression difference can be captured and compared on MR with specific targeted probe. Tenascin-C targeted MRI can provide more accurate information for the occurrence of cervical cancer, preoperative cancer invasiveness evaluation and prognosis.

Development of metastasis requires not only cancer cell: increase motility and invasiveness, entry and survival in blood circulation and resistant to autoimmunity.[13] But also supportive signals from the surrounding microenvironment.[14] Tenascin-C's function is noteworthy and spans activities such as regulation of adhesion and migratory mechanisms, promotion of angiogenesis and modulation of immune responses.[15,16] The upregulation of tenascin-C in the cancer microenvironment can facilitate stromal formation and promote metastatic colonization.[17,18] Hence, many reports have suggested a supportive role for tenascin-C in tumor metastasis. Weidong Ni et al reported that tenascin-C in prostate cancer stromal was significantly correlated with lymph node metastasis and clinical stage.[19] But the tenascin-C expression with lymph node metastasis in cervical cancer has not been researched before. Tenascin-C has been proved to increase in invasive cervical cancer but showed no value in distinguishing various cervical intraepithelial neoplasia grades.[20,21] We think the importance of tenascin-C expression difference is in detecting malignant cervical cancer and in distinguishing cancer invasiveness. Our research showed highest expression of tenascin-C in cervical cancer tissues with lymph node metastasis compared with cervical cancer tissues without metastasis and normal cervix.

Figure 5. MR signal decrement comparison among the three groups. Group A: cervical cancer with lymph node metastasis showed highest signal decrease. Group B: cervical cancer without lymph node metastasis showed moderate signal decrease. Group C: normal cervix showed least signal decrease. CNR, contrast-to-noise ratio.

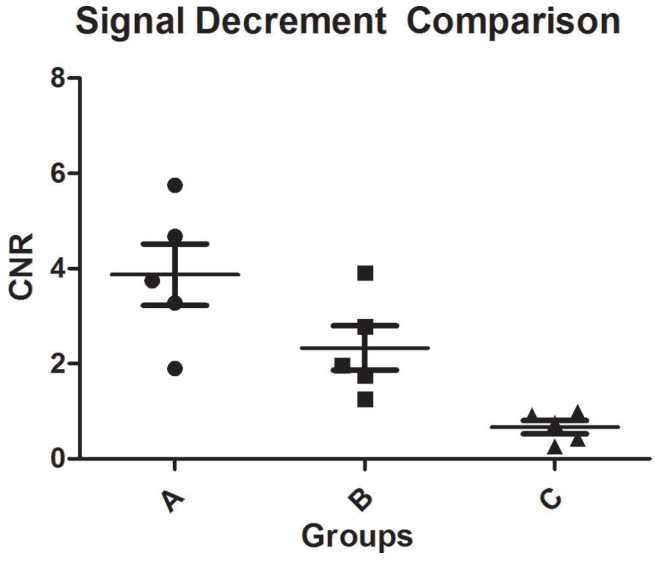

Lymph node metastasis detection influences treatment and affects 5-year survival rate.[22] There are many kinds of methods to assess lymph node metastasis in cervical cancer patients. Blue dyes and ^{99}Tc have been used for mapping with sentinel lymph node biopsy in cervical cancer, with an overall sensitivity and sentinel lymph node detection rate of over 90 %.[23] However, blue dyes cause discoloration of skin and urine, a decrease in pulse oximetry readings and, occasionally, severe allergic reactions.[24,25] ^{99}Tc is radioactive and rather complicated.[26] Photon emission CT (PET/CT) is another commonly used method, but the efficacy is not established and has limitations associated with the correct region of metastatic lymph node.[27] Tenascin-C is a protein not used to show the accurate location of the metastatic nodes, but to detect the invasive cervical cancer with a higher metastatic potential. Then, lymphadenectomy is recommended even though the node is not enlarged on MR.

Since tenascin-C is a marker for lymph node metastasis in cervical cancer. Then, how to easily capture this marker on visible images is of great practical value. One paper researched radiolabeled tenascin-C with (18)F and (64)Cu provided clear visualization of the tumor in mice.[28] This provided a photon emission tomography imaging method with tenascin-C. For cervical cancer, MRI is the most commonly used method: such as stage the primary tumor, monitor response to treatment, detect recurrence, and in radiotherapy planning.[29] Therefore, we focused on MR targeted imaging and extend the expression level with tumor invasiveness. MR probe targeted tenascin-C can not only depict the original cervical cancer, but also move forward to signal out the metastatic lymph node. This molecular targeted imaging can help to pick out the cervical cancer patients with difficulty in preoperative tumor sampling or with negative pathology results. The operative strategy can be considered together with the tenascin-C expression level and MR signal changes. In future clinical

imaging, convention MR results including tumor size, location, border and enhancement should be considered together with molecular targeted imaging results including tumor cell viability, invasion and metastatic potential. In order to offer a more comprehensive information for therapeutic strategy.

There were some limitations in our study. Firstly, the number of research tissues is not large enough. This is a preliminary tentative research for future larger samples. We are going to collecting more cases and calculate the signal threshold to offer more useful clinical information. Secondly, the imaging of the tumor is *in vitro*. Tumor environment and probe targeted combination may be different from *in vivo*. However, the tumor tissues might be regarded as fresh. Because we incubated the tissues with probes directly after surgery under 37°C. And, our group will continue to implant subcutaneous tumor in mice and do *in vivo* imaging.

CONCLUSION

Tenascin-C is a sensitive marker to evaluate cervical cancer. With the specific SPIO-antitenascin-C probe, MRI can be a noninvasive method to depict cervical cancer with node metastasis.

REFERENCES

1. Midwood KS, Hussenet T, Langlois B, Orend G. Advances in tenascin-C biology. *Cell Mol Life Sci* 2011; **68**: 3175–99. doi: https://doi.org/10.1007/s00018-011-0783-6
2. Hancox RA, Allen MD, Holliday DL, Edwards DR, Pennington CJ, Guttery DS, et al. Tumour-associated tenascin-C isoforms promote breast cancer cell invasion and growth by matrix metalloproteinase-dependent and independent mechanisms. *Breast Cancer Res* 2009; **11**: R24. doi: https://doi.org/10.1186/bcr2251
3. Juuti A, Nordling S, Louhimo J, Lundin J, Haglund C. Tenascin C expression is upregulated in pancreatic cancer and correlates with differentiation. *J Clin Pathol* 2004; **57**: 1151–5. doi: https://doi.org/10.1136/jcp.2003.015818
4. Hirata E, Arakawa Y, Shirahata M, Yamaguchi M, Kishi Y, Okada T, et al. Endogenous tenascin-C enhances glioblastoma invasion with reactive change of surrounding brain tissue. *Cancer Sci* 2009; **100**: 1451–9. doi: https://doi.org/10.1111/j.1349-7006.2009.01189.x
5. Chuanyu S, Yuqing Z, Chong X, Guowei X, Xiaojun Z. Periostin promotes migration and invasion of renal cell carcinoma through the integrin/focal adhesion kinase/c-Jun N-terminal kinase pathway. *Tumour Biol* 2017; **39**: 101042831769454. doi: https://doi.org/10.1177/1010428317694549
6. Jones FS, Burgoon MP, Hoffman S, Crossin KL, Cunningham BA, Edelman GM. A cDNA clone for cytotactin contains sequences similar to epidermal growth factor-like repeats and segments of fibronectin and fibrinogen. *Proc Natl Acad Sci U S A* 1988; **85**: 2186–90. doi: https://doi.org/10.1073/pnas.85.7.2186
7. Buyukbayram H, Arslan A. Value of tenascin-C content and association with clinicopathological parameters in uterine cervical lesions. *Int J Cancer* 2002; **100**: 719–22. doi: https://doi.org/10.1002/ijc.10546
8. Tiitta O, Wahlström T, Paavonen J, Linnala A, Sharma S, Gould VE, et al. Enhanced tenascin expression in cervical and vulvar koilocytotic lesions. *Am J Pathol* 1992; **141**: 907–13.
9. Kodama J, Seki N, Nakamura K, Hongo A, Hiramatsu Y. Prognostic factors in pathologic parametrium-positive patients with stage IB-IIB cervical cancer treated by radical surgery and adjuvant therapy. *Gynecol Oncol* 2007; **105**: 757–61. doi: https://doi.org/10.1016/j.ygyno.2007.02.019
10. Rockall AG, Qureshi M, Papadopoulou I, Saso S, Butterfield N, Thomassin-Naggara I, et al. Role of imaging in fertility-sparing treatment of gynecologic malignancies. *Radiographics* 2016; **36**: 2214–33. doi: https://doi.org/10.1148/rg.2016150254
11. Scheidler J, Hricak H, Yu KK, Subak L, Segal MR. Radiological evaluation of lymph node metastases in patients with cervical cancer. A meta-analysis. *JAMA* 1997; **278**: 1096–101. doi: https://doi.org/10.1001/jama.1997.03550130070040
12. Klerkx WM, Veldhuis WB, Spijkerboer AM, van den Bosch MA, Mali WP, Heintz AP, et al. The value of 3.0Tesla diffusion-weighted MRI for pelvic nodal staging in patients with early stage cervical cancer. *Eur J Cancer* 2012; **48**: 3414–21. doi: https://doi.org/10.1016/j.ejca.2012.06.022
13. Gupta GP, Massagué J. Cancer metastasis: building a framework. *Cell* 2006; **127**: 679–95. doi: https://doi.org/10.1016/j.cell.2006.11.001
14. Vanharanta S, Massagué J. Origins of metastatic traits. *Cancer Cell* 2013; **24**: 410–21. doi: https://doi.org/10.1016/j.ccr.2013.09.007
15. Yoshida T, Akatsuka T, Imanaka-Yoshida K. Tenascin-C and integrins in cancer. *Cell Adh Migr* 2015; **9**: 96–104. doi: https://doi.org/10.1080/19336918.2015.1008332
16. Lowy CM, Oskarsson T. Tenascin C in metastasis: a view from the invasive front. *Cell Adh Migr* 2015; **9**: 112–24. doi: https://doi.org/10.1080/19336918.2015.1008331
17. Tamaoki M, Imanaka-Yoshida K, Yokoyama K, Nishioka T, Inada H, Hiroe M, et al. Tenascin-C regulates recruitment of myofibroblasts during tissue repair after myocardial injury. *Am J Pathol* 2005; **167**: 71–80. doi: https://doi.org/10.1016/S0002-9440(10)62954-9
18. O'Connell JT, Sugimoto H, Cooke VG, MacDonald BA, Mehta AI, LeBleu VS, et al. VEGF-A and Tenascin-C produced by S100A4+ stromal cells are important for metastatic colonization. *Proc Natl Acad Sci U S A* 2011; **108**: 16002–7. doi: https://doi.org/10.1073/pnas.1109493108
19. Ni WD, Yang ZT, Cui CA, Cui Y, Fang LY, Xuan YH. Tenascin-C is a potential cancer-associated fibroblasts marker and predicts poor prognosis in prostate cancer. *Biochem Biophys Res Commun* 2017; **486**: 607–12. doi: https://doi.org/10.1016/j.bbrc.2017.03.021
20. Iskaros BF, Koss LG. Tenascin expression in intraepithelial neoplasia and invasive carcinoma of the uterine cervix. *Arch Pathol Lab Med* 2000; **124**: 1282–6. doi: https://doi.org/10.1043/0003-9985(2000)124<1282:TEIINA>2.0.CO;2
21. Pöllänen R, Soini Y, Vuopala S, Läärä E, Lehto VP. Tenascin in human papillomavirus associated lesions of the uterine cervix. *J Clin Pathol* 1996; **49**: 521–3. doi: https://doi.org/10.1136/jcp.49.6.521
22. Choi HJ, Kim SH, Seo SS, Kang S, Lee S, Kim JY, et al. MRI for pretreatment lymph node staging in uterine cervical cancer. *AJR Am J Roentgenol* 2006; **187**:

W538–W543. doi: https://doi.org/10.2214/AJR.05.0263

23. Rob L, Lukas R, Robova H, Helena R, Halaska MJ, Jiri HM, Hruda M, Skapa P, et al. Current status of sentinel lymph node mapping in the management of cervical cancer. *Expert Rev Anticancer Ther* 2013; **13**: 861–70. doi: https://doi.org/10.1586/14737140.2013.811147
24. Kieckbusch H, Coldewey SM, Hollenhorst J, Haeseler G, Hillemanns P, Hertel H. Patent blue sentinel node mapping in cervical cancer patients may lead to decreased pulse oximeter readings and positive methaemoglobin results. *Eur J Anaesthesiol* 2008; **25**: 365–8. doi: https://doi.org/10.1017/S0265021508003578
25. Bricou A, Barranger E, Uzan S, Darai E. Anaphylactic shock during the sentinel lymph node procedure for cervical cancer. *Gynecol Oncol* 2009; **114**: 375–6. doi: https://doi.org/10.1016/j.ygyno.2009.04.027
26. Imboden S, Papadia A, Nauwerk M, McKinnon B, Kollmann Z, Mohr S, et al. A comparison of radiocolloid and indocyanine green fluorescence imaging, sentinel lymph node mapping in patients with cervical cancer undergoing laparoscopic surgery. *Ann Surg Oncol* 2015; **22**: 4198–203. doi: https://doi.org/10.1245/s10434-015-4701-2
27. Nogami Y, Banno K, Irie H, Iida M, Kisu I, Masugi Y, et al. The efficacy of preoperative positron emission tomography-computed tomography (PET-CT) for detection of lymph node metastasis in cervical and endometrial cancer: clinical and pathological factors influencing it. *Jpn J Clin Oncol* 2015; **45**: 26–34. doi: https://doi.org/10.1093/jjco/hyu161
28. Jacobson O, Yan X, Niu G, Weiss ID, Ma Y, Szajek LP, et al. PET imaging of tenascin-C with a radiolabeled single-stranded DNA aptamer. *J Nucl Med* 2015; **56**: 616–21. doi: https://doi.org/10.2967/jnumed.114.149484
29. Fridsten S, Hellström AC, Hellman K, Sundin A, Söderén B, Blomqvist L. Preoperative MR staging of cervical carcinoma: are oblique and contrast-enhanced sequences necessary? *Acta Radiol Open* 2016; **5**: 2058460116679460. doi: https://doi.org/10.1177/2058460116679460